THE INFLUENCE OF MICROSTRUCTURE ON THE HYDROGEN INDUCED CRACKING SUSCEPTIBILITY OF HIGH STRENGTH STEEL

B.Ule*, F.Vodopivec*, L.Kosec**

The use of notched specimens is described for study of delayed fracture caused by stress-induced hydrogen segregation in high strength steel.
Measurements of the critical and of the threshold stress intensity factor are presented which represent the basis for analysing the influence of small microstructural variations of steel on its sensitivity to the delayed fracture.

INTRODUCTION

Delayed failure caused by stress-induced hydrogen segregation in steel can be divided into three stages: first crack nucleation, then slow crack growth and finally rapid unstable fracture.

Dissolved hydrogen, being a particularly mobile interstitial solute, is very apt to achieve the necessary inhomogeneous distribution for uniform chemical potencial in an inhomogeneous elastic stress field, for instance at the notch root.

The critical concentration of hydrogen which produces crack nucleation at the distance r from the notch root can be achieved only if the applied stress intensity factor K_I is higher than the threshold stress intensity factor K_{TH}.

* Institute of metallurgy, Ljubljana, Yugoslavia
** University Edvard Kardelj, Ljubljana, Yugoslavia

According to Gerberich (1) the following equation can be written:

$$K_{TH} = \frac{RT}{\alpha \bar{V}_H} \ln \frac{[H]_r^{cr}}{[H]} - \frac{\sigma_{ys}}{2\alpha} \quad \ldots (1)$$

For notched tensile specimens with the geometry shown in Fig.1 the relationship between the stress intensity factor K_I, the geometry and the axial force P is given by the equation (2):

$$K_I = \frac{P}{D^{3/2}} (-1,27 + 1,72\ D/d) \ldots\ldots (2)$$

under condition that: $0,5 < d/D < 0,8$

Moran and Norris (3) found by the computer simulation of the tension test with notched specimens, that the maximum stresses at fracture occur at about two notch-root radii below the surface when the ρ/D ratio is 0,01 to 0,02. On the other hand the maximum strain occurs at the notch root where also the first microcracks appear.

EXPERIMENTS AND RESULTS

Selection of Steel. The aim of investigation was to establish the influence of microstructure on the hydrogen induced susceptibility to cracking of a high-strength steel with 0,40 % C, 1,03 % Cr and 0,21 % Mo. The initial hydrogen content did not exceed 0,05 ppm.

Thermal Treatment. Peripherally notched cylindrical specimens were austenitized 30 mins. at 850 °C, quenched in water or in oil and tempered.

Fig.2 shows the microstructure of the lath martensite in steel quenched in water. After tempering 2 hrs. at 480 °C or 420 °C yield strengths of 1185 and 1290 Nmm^{-2} respectively were obtained.

The hardness of oil quenched specimens reached only 52 HRc, which means, that the predominantly martensitic microstructure of

oil quenched specimens still contains up to 5 % of bainite (Fig.3). After tempering specimens quenched in oil 2 hrs. at 450 °C, a yield strength of 1230 Nmm^{-2} was obtained.

Hydrogen Charging. After thermal treatment, the specimens were charged with hydrogen by etching 24 hrs. in a 0,1 N aqueous solution of hydrochloric acid.

Chemical analysis of specimens immediately after the removal from the acid solution showed a hydrogen concentration of 2,9 ± 0,1 ppm independently of the yield strength of steel. It was concluded that all the traps were not saturated since in such a case the concentration of hydrogen in steel would be different in samples with different yield strength (4).

Twenty-four hours after removal from the acid solution, the concentration of hydrogen in specimens dropped to 0,82 ± 0,1 ppm and after 48 hours to 0,58 ± 0,08 ppm, which was assumed to be the residual concentration.

Determination of the Critical and the Threshold Stress Intensity Factor

An experimental set-up was developed for the registration of the incubation period as well as for the registration of the slow propagation of microcracks to the instantaneous fracture of the round-notched specimens under static load. This experimental set-up, which consisted of a half-Wheatston bridge with a variable resistor represented by a strain-gauge sticked across the notch opening, permitted to detect the propagation steps of about 0,1 μm.

An almost similar set-up was used to measure the critical stress intensity factor K_{Ic} of steel. Fig.4 shows how measurements were made on the "Instron" tensile machine with an accurate extensometer mounted on the notch opening of the specimen for calibration of the strain-gauges. Some more details of this technique are given in reference (5).

The threshold stress intensity factor K_{TH} was experimentally determined by measuring the time till fracture occurs related to the applied static load, whereas the critical stress intensity factor K_{Ic} was measured on round notched tensile specimens with fatigue crack at the notch tip. The Eq. (2) was applied to calculate both the threshold and the critical stress intensity factor. The width of the fatigue crack was measured with an optical microscope after each experiment.

The relation between the measured factors (K_{TH}, K_{Ic}) and the yield strength of the investigated steel is shown in Fig.5.

The threshold stress intensity factor K_{TH} for tempered martensitic-bainitic microstructure (point M+B) has the same value as that for fully martensitic tempered microstructure with the same yield strength.

Hydrogen has no noticeable influence, if any at all, on the fracture toughness of the investigated steel. However, at the same yield strength, the fracture toughness, contrary to the threshold stress intensity factor, depends slightly on small microstructure variations of steel.

Micromorphology of Fractures. Microfractographic investigations of fracture surfaces of round notched tensile specimens, charged with hydrogen, were performed in a scanning electron microscope.

Fig.6 shows a slow crack propagation area of fracture surface of a round notched tensile specimen with fully martensitic tempered microstructure and yield strength 1185 Nmm^{-2}. Static load i.e. applied stress intensity factor 2190 $Nmm^{-3/2}$ was close to the limiting value (K_{TH} = 2180 $Nmm^{-3/2}$) which caused the delayed fracture of the specimen after 181 hours.

The fracture area near the notch tip is predominantly ductile although irregularly shaped dimples are found next to the well - defined dimples.

Fig.7 indicates representative crack configurations at the longitudinal section in notched specimen which had been unloaded

before delayed failure occurred. The comparison of this photo with the slip line field for a circular stress-free boundary (Fig.8) shows that the slip line directions i.e. directions of pure shear strain and crack paths are essentially coincident.

CONCLUSIONS

Measurements of the threshold stress intensity factor K_{TH} of the hydrogen charged chromium-molibdenum high strength steel with the tempered martensitic microstructure or the tempered martensitic - bainitic microstructure and with the same yield strength showed that small microstructure variations of the investigated steel had no influence on K_{TH}.

These results confirm the Nakasato´s and Terasaki´s statements (6) according to which the threshold stress intensity factor K_{Iscc} at the same tensile strength does not depend on the microstructure variations of high strength steel. If this statement is general, the hypothesis suggesting that the microcrack nucleation leading to the delayed fracture is always confined to martensitic areas of the microstructure ($[H]^{cr}$ is at first reached) has argument. It seems that this is the only way to explain the lack of influence of small portion of bainite in a predominantly martensitic microstructure of the tempered high strength steel on the threshold stress intensity factor.

The measurements of the critical stress intensity factor show that small concentrations of hydrogen in the investigated steel has no noticeable influence on the fracture toughness of steel. However, at the same yield strength the fracture toughness - contrary to the threshold stress intensity factor - depends also on small microstructure variations of steel, since steel with the tempered martensitic-bainitic microstructure has a slightly higher fracture toughness than the same steel with the tempered martensitic microstructure and with the same yield strength. The results of this investigation agree with data published by Ohtani et al (7) who

explained this phenomenon by the beneficial effect of a small quantity of bainite which reduces the size of single austenite-grain parts in which the martensitic transformation takes place. Such a microstructure could be less sensitive to the delayed fracture.

The nucleation of the first crack in the region of maximal strain at the notch tip as well as the predominantly ductile type of fracture in that area suggest the conclusion that the nucleation of microcracks is a strain-induced process resulting from the decreasing fracture ductility which occurs during the static delayed fracture test.

SYMBOLS USED

D = outer diameter of tensile specimen (mm)

d = diameter of the notched part of specimen (mm)

$[H]^{cr}$ = critical hydrogen concentration (ppm)

$[H]$ = average hydrogen concentration (ppm)

K_{TH} = threshold stress intensity factor ($Nmm^{-3/2}$)

K_{Ic} = critical stress intensity factor ($Nmm^{-3/2}$)

P = tensile load (N)

R = gas constant (8.314 J mol^{-1} K^{-1})

T = absolute temperature (K)

$\bar{V}_H$ = partial atomic volume of hydrogen in iron (cm^3 $g\text{-}atom^{-1}$)

σ_{ys} = yield strength (Nmm^{-2})

ρ = notch root radius (mm)

α = constant in Gerberich's (1) equation

REFERENCES

(1) Gerberich,W.W.,"Effect of hydrogen in high-strength and martensitic steels",Hydrogen in Metals,ASM - Ohio, USA, 1974.

(2) Heckel,K.,"Einführung in die technische Anwendung der Bruchmechanik", Carl Hauser Verlag, München, W.Germany, 1970, pp. 33-34.

(3) Moran,B. and Norris,D.M., Metallurgical Transactions A, Vol.9A, 1978, pp. 1685-1687.

(4) Kim,C.D. and Loginow,A.W., Corrosion-Nace, Vol.24, No.10, 1968, pp. 313-318.

(5) Ule,B.,Vodopivec,F.,Žvokelj,J.,Grašič,M. and Kosec,L., Železarski zbornik, Vol.21, No.4, 1987, pp. 183-191.

(6) Nakasato,F. and Terasaki,F., Transactions ISIJ, Vol.15, 1975, pp. 290.

(7) Ohtani,H.,Terasaki,F. and Kunitake,T., Transactions ISIJ, Vol.12, 1972, pp. 118-127.

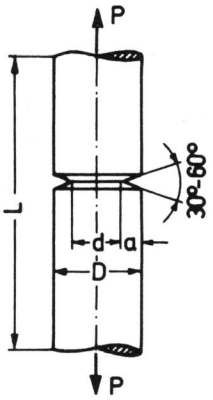

Figure 1 Round notched tensile specimen

Figure 2 Lath-shaped martensite

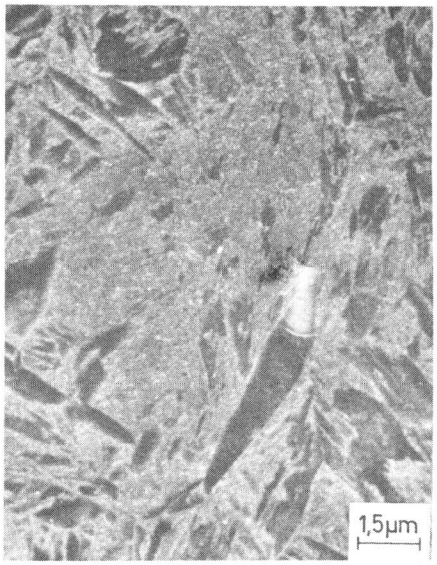

Figure 3 Lower bainite in the martensitic matrix

Figure 4 Experimental set-up for measurement of K_{Ic}

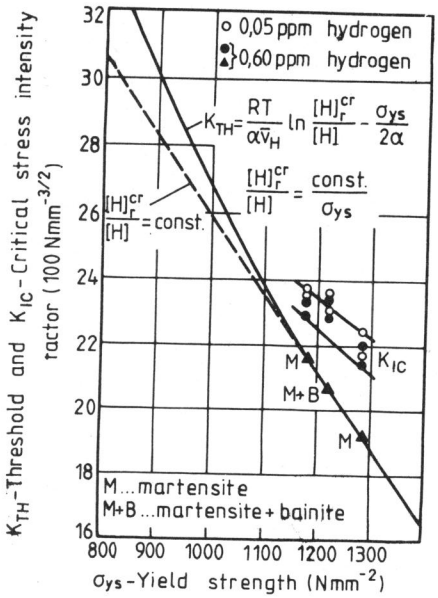

Figure 5 Stress intensity factors vs. yield strength

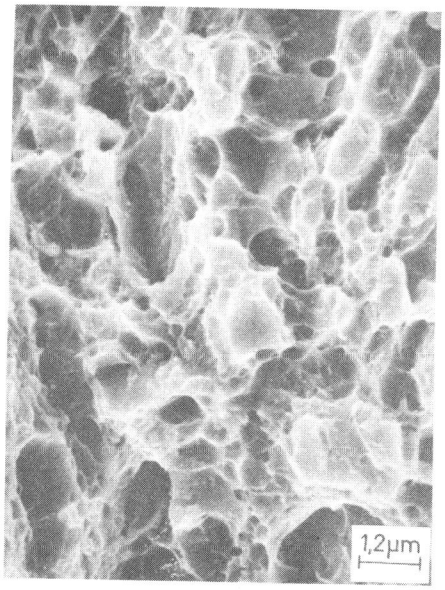

Figure 6 Ductile fracture in slow crack region

Figure 7 Nucleated microcracks at the notch tip

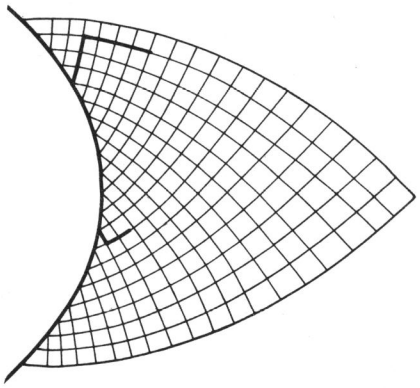

Figure 8 Slip line field at the notch tip with cracks